Mat. Res. Soc. Symp. Proc. Vol. 706 © 2002 Materials Research Society

G-band Raman Spectra of Isolated Single Wall Carbon Nanotubes: Diameter and Chirality Dependence

A. Jorio[a], A. G. Souza Filho[a,b], G. Dresselhaus[a], M. S. Dresselhaus[a], A. K. Swan[c], M. S. Ünlü[c], B. B. Goldberg[c], M. A. Pimenta[d], J. H. Hafner[e], C. M. Lieber[e], and R. Saito[f]

[a]Massachusetts Institute of Technology, Cambridge, MA 02139-4307 USA;
[b]Univ. Federal do Ceará, Fortaleza, CE 60455-760 Brazil;
[c]Boston Univ., Boston, MA 02215 USA;
[d]Univ. Federal de Minas Gerais, Belo Horizonte, MG 30123-970 Brazil;
[e]Harvard Univ., Cambridge, MA 02138, USA;
[f]Univ. of Electro-Communications, Tokyo, 182-8585 Japan;

ABSTRACT

We present results from resonant Raman spectroscopy on the graphite-like G band by measuring Raman spectra on isolated single wall carbon nanotubes (SWNTs). We discuss the G-band lineshape dependence on nanotube diameter and chirality, as well as polarization studies related to the antenna effect. Symmetry selection rules, dipolar and multipolar antenna behaviors are discussed. Spectra at the single nanotube level are related to spectra observed from SWNT bundles.

INTRODUCTION

Raman scattering is well known as an important technique to characterize the different forms of carbon materials.[1] Recently, the resonant Raman scattering (RRS) technique has been shown to provide a powerful tool for studying and characterizing single wall carbon nanotubes (SWNTs), first for SWNT bundles [2] and recently for isolated SWNTs.[3, 4, 5, 6] These carbon-made cylinders with nano-metric diameters exhibit two main features in the first-order Raman spectra: the radial breathing mode (RBM) and the tangential mode vibrations (forming the so-called G band). The resonant Raman spectra of the RBMs ($A\,(A_{1g})$ symmetry) provide an easy and quick determination of the tube diameter distribution present in SWNT bundles [2] or the (n, m) identification of an isolated SWNT.[3] The G band is related to the graphite Raman-active E_{2g_2} mode, but in SWNTs the G band appears to be a more complex spectral feature, composed of six modes, two of each of the symmetries: $A\,(A_{1g})$, $E_1\,(E_{1g})$ and $E_2\,(E_{2g})$.[2] The splitting of the E_{2g_2} graphite mode into many peaks for SWNTs is due to the zone folding of the graphite 3D Brillouin zone into the 1D SWNT Brillouin zone, and due to the lowering of the symmetry through nanotube curvature, thus distinguishing the axial and circumferential directions, and giving us important information about the confinement of the phonon structure in this 1D material. The G-band spectra for graphite, for one semiconducting SWNT and for one metallic SWNT are shown in Fig. 1(a). Another important characteristic of the G-band feature is the difference in lineshape between metallic and semiconducting SWNTs [2], as shown in Fig. 1(a), allowing the use of resonance Raman scattering for materials characterization.

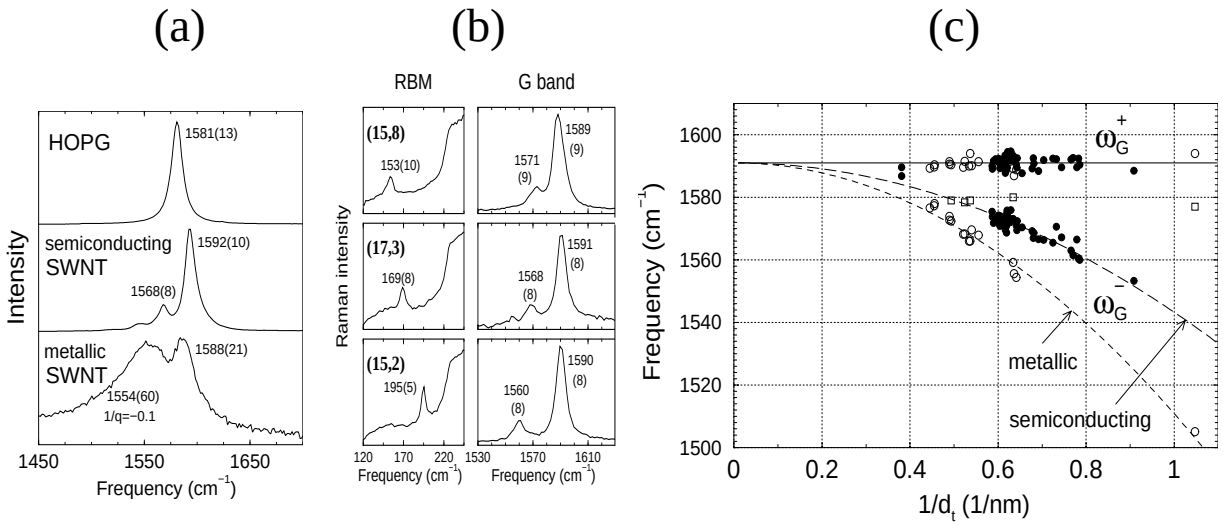

Figure 1: (a) The G-band for graphite, one semiconducting SWNT and one metallic SWNT. (b) RBM and G-band Raman spectra for three semiconducting isolated SWNTs.(c) Frequency vs. $1/d_t$ for the two most intense G-band features (ω_G^- and ω_G^+) from isolated SWNTs.

So far, most of the experimental results on the G-band spectra of SWNTs come from SWNT bundles. Although there have been a considerable number of studies on the G-band feature regarding the difference in behavior between metallic and semiconducting nanotubes, and regarding the dependence of the G band spectra on polarization scattering geometries [2], very little is known about the dependence of the G-band spectra on nanotube structure, i.e., on diameter d_t and chiral angle θ, or about their polarization behavior at the isolated SWNT level. Studies of the d_t dependence of the G-band mode frequencies were previously performed for both semiconducting [7] and metallic [8] SWNTs contained in bundles. However, since the SWNT bundles often exhibit a distribution of tube diameters (more than 10 %), and very few different bundles have been measured so far (only 3 samples of SWNT bundles with different d_t distributions) [7, 8], the results were not definitive. Chirality information is obviously not provided by bundle measurements. The general polarization behavior of aligned SWNTs in bundles is determined by the "depolarization" (or "antenna") effect, whereby light scattering is suppressed for light polarized perpendicular to the tube axes.[4]

We summarize here the resonant Raman spectra of the graphite-like G band obtained from 62 isolated SWNTs, including the G band lineshape dependence on nanotube diameter and chirality, as well as polarization studies, revealing not only the usual dipolar antenna effect, but also multipolar antenna behavior. We relate results at the single nanotube level to spectra observed from SWNT bundles.

EXPERIMENTAL DETAILS

In this work we only discuss isolated SWNTs resonant with the *incident* light, so that all the SWNT Raman features appear in the single nanotube spectra, and we can then use the tentative (n, m) assignment from the RBM, D-band and G'-band Raman features to analyze the G-band spectra systematically.[3, 5, 6] The use of a very dilute sample ($\sim 0.4\,\mathrm{SWNT}/\mu\mathrm{m}^2$) is important to be sure that when we observe, for example, the RBM

feature and the G band in the same laser spot, both of these features come from the same SWNT. By imaging the sample with atomic force microscopy, good spatial isolation between SWNTs is observed, although a very few of them ($< 10\%$) are found to be close enough to each other to be illuminated in one laser spot ($\sim 1\,\mu$m) at the same time. Results from the Raman spectra from *62 different isolated SWNTs* (46 semiconducting and 16 metallic SWNTs), resonant with the incident laser light, are summarized here.

Isolated SWNTs were prepared by a chemical vapor deposition method on a Si/SiO_2 substrate.[3] The Raman spectra were obtained using two Raman systems: a single monochromator Renishaw 1000B spectrometer equipped with a cooled CCD detector and notch filters, and a Kaiser Optical System, Hololab 5000R: Modular Research Micro-Raman Spectrograph. The Raman spectra were collected in a back scattering configuration by a microscope using a 100× objective (laser spot $\sim 1\,\mu$m). Three laser lines [514.5 nm (2.41 eV) and 488.0 nm (2.54 eV) from an Ar ion laser, and 785 nm (1.58 eV) from a Ti:Sapphire laser] were used to obtain the Raman spectra from both metallic and semiconducting SWNTs over the diameter range present in the sample ($0.9 < d_t < 3.0$ nm). Polarization studies were performed using a $\lambda/2$ plate situated close to the sample, to rotate both the incident and back-scattered light.

RESULTS AND DISCUSSIONS

Figure 1(a) shows the G band for graphite, a semiconducting SWNT, and a metallic SWNT. The Raman spectrum from graphite exhibits a single Lorentzian peak at $1581\,\mathrm{cm}^{-1}$, corresponding to the E_{2g_2} symmetry mode. For SWNTs, this band splits into several features due to the 1D quantum confinement of the phonons. In the case of semiconducting SWNTs four Lorentzian-shape peaks are observed, with the two most intense features shown at $\omega_G^- = 1568\,\mathrm{cm}^{-1}$ $\omega_G^+ = 1592\,\mathrm{cm}^{-1}$. For metallic SWNTs, the lower frequency feature ω_G^- exhibits a Breit-Wigner-Fano (BWF) lineshape. The asymmetric SWNT lineshape has previously been used to fit some Raman bands for the metallic forms of various sp^2 carbons (e.g. alkali-metal graphite intercalation compounds, K_3C_{60} and carbon aerogels).[8]

Figure 1(b) shows the RBM and the G-band Raman spectra for three semiconducting isolated SWNTs. The G-band spectra are typical of SWNT bundles [2], but the spectra for isolated nanotubes exhibit much smaller line widths ($9\,\mathrm{cm}^{-1}$ compared to $20\,\mathrm{cm}^{-1}$ in SWNT bundles). The spectra are displayed, from top to bottom, according to increasing RBM frequency (ω_{RBM}), i.e., according to decreasing SWNT diameter (d_t). The G-band linewidth does not exhibit a diameter dependence for this d_t range.

In Fig. 1(c) we plot the frequency vs. $1/d_t$ for the two most intense G-band features (ω_G^- and ω_G^+) from isolated SWNTs studies.[9] Filled circles are for semiconducting tubes and open circles are for metallic tubes. The upper frequency ω_G^+ does not show a d_t dependent behavior, but always appears at about $1591\,\mathrm{cm}^{-1}$ for the SWNT d_t range of the SWNTs in our sample. This is in agreement with several different resonance Raman measurements on SWNT bundles.[2] The lower frequency ω_G^- mode, however, shows a diameter dependence that can be very well fit with a simple equation $\omega_G^- = \omega_G^+ - C_S/d_t^2$, with the constants $C_{\mathrm{S}} = 47.7\,\mathrm{cm}^{-1}\mathrm{nm}^2$ for semiconducting SWNTs and $C_{\mathrm{S}} = 79.5\,\mathrm{cm}^{-1}\mathrm{nm}^2$ for metallic SWNTs.[9] The diameter dependence of the G-band modes presented in Fig. 1(c) can be used to analyze the dispersion of frequencies of the G-band in SWNT bundles, as well as the average diameter distribution.

Previous polarization studies show that the two most intense G-band features ω_G^- and ω_G^+ are composed of A and E_1 symmetry modes.[11] Molecular dynamics (von Karaman

force) method [15] shows that the splitting between ω_G^- and ω_G^+ can be explained as due to a lowering of the symmetry, thereby distinguishing the axial and circumferential directions. The force constants for the ω_G^- modes with atomic vibrations along the circumferential direction are strongly dependent on nanotube curvature, while the force constants for the ω_G^+ modes, where the atomic vibrations occur along the tube axis direction, would not depend on d_t. The curvature results in an out-of-plane component for the circumferential vibrations, which lowers the frequency. Note that at the Γ point of graphite, the in-plane vibrations have a frequency of $1580\,\mathrm{cm}^{-1}$, while the out-of-plane vibration appears at about $860\,\mathrm{cm}^{-1}$. Regarding metallic SWNTs, the observation of the BWF coupling only for the low frequency mode can also be understood based on circumferential vs. axial atomic vibrations, where the out-of-plane component for the circumferential vibrations is responsible by the electron-phonon coupling.[8] The extra downshift of the BWF peak in metallic SWNTs, compared to semiconducting SWNTs, is attributed to the phonon-plasmon coupling in the metallic SWNTs, and it increases by increasing the nanotube curvature.[8]

Recent *ab initio* calculations of the vibrational properties of SWNTs lead to the conclusion that the phonon eigenvectors can only be differentiated in the axial and circumferential directions in the case of the high symmetry achiral SWNTs, but in the case of chiral SWNT, the atomic bondings (i.e. chiral angle) drive the direction of the atomic vibrations.[10] However, the dispersive/non-dispersive behavior of the ω_G^-/ω_G^+ peaks in the G band of both metallic and semiconducting SWNTs clearly show, from an experimental point of view, that ω_G^- and ω_G^+ exhibit different behaviors from each other, and that nanotube curvature is more important than nanotube chirality for determining ω_G^- and ω_G^+.

We also studied the polarization dependence of the resonance Raman spectra for several other isolated single wall carbon nanotubes (SWNTs). Each isolated SWNT acts as a dipolar antenna, polarized along its tube axis. For light polarized parallel to the tube axis, the strong resonance effect is seen to break the symmetry selection rules, and symmetry-forbidden modes can be seen in the Raman spectrum.[2] When the light is not polarized parallel to the tube axis, the constituent G-band mode symmetries can then be identified. Figure 2(b) shows the increase in relative intensity for the highest and lowest frequency modes [indicated by arrows in Fig. 2(b)] when the incident and scattered light become polarized perpendicular to the tube axis ($\phi = 90°$). This result is in agreement with group theory predictions for the E_2 modes and with previous polarization studies on SWNT bundles.[11]

Unusual G-mode intensity behaviors are observed rarely, and can be seen when the polarized Raman signals are obtained from two or more isolated SWNTs that are close to each other, or even cross each other, so that they can be illuminated at the same light spot. Such unusual G-mode intensity behaviors are illustrated in Figs.2(c) and (d) and suggest a complex multipolar antenna pattern. Different unusual G-band intensity polarization behaviors were observed for different light spots with two resonant SWNTs. This result indicates that different nanotubes with different spatial arrangements (different origin and axes orientations) give different multipolar antenna patterns. The identification of this unusual polarization behavior with the presence of more than one SWNT within the same light spot is confirmed by measuring the polarization behavior of SWNT samples with a larger density of tubes on the Si/SiO_2 substrate. In such larger density samples, unusual behaviors of this kind are observed more often. More work is necessary to understand this complicated multipolar antenna effect. The usual dipolar antenna effect can provide the orientation of an isolated SWNT, and the understanding of this multipolar antenna behavior may give us a powerful tool for the spatial characterization of tubes that are close

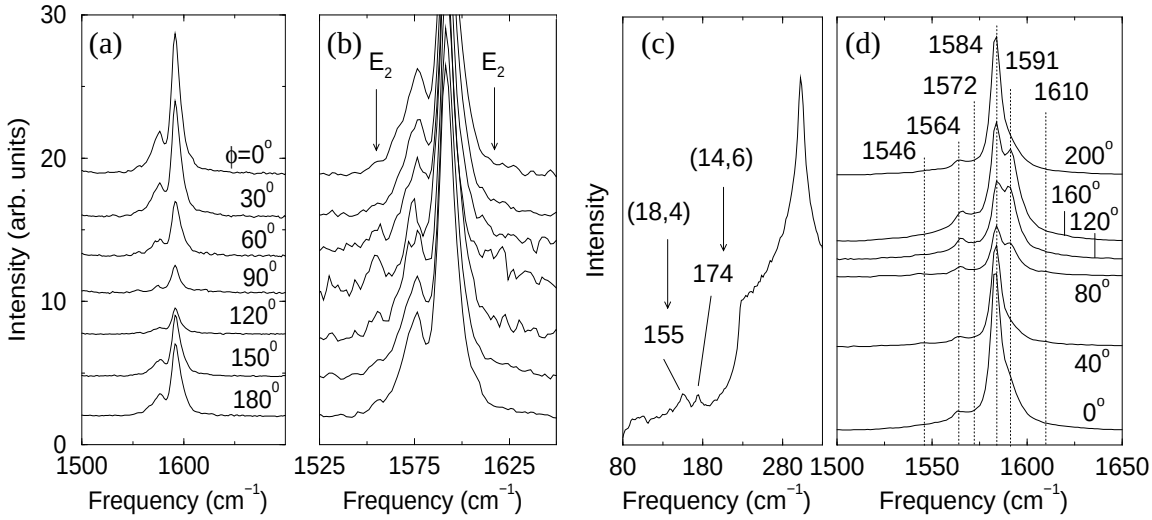

Figure 2: (a) (VV) G-band Raman spectra from one light spot on the sample, taken with different angles ϕ (see text). (b) The same spectra as (a) but with normalized intensity. (c) RBM spectra from a different spot on the sample than (a) and (b). (d) (VV) G-band Raman spectra from the same light spot as (c), taken with different angles ϕ. The peak frequencies are displayed in cm^{-1}.

to each other.

These results can explain contradictory experimental results in the literature about polarization Raman studies on carbon nanotube bundles. Some papers on thin aligned SWNT bundles show that the polarization dependence of the Raman signal exhibits the simple dipolar antenna behavior.[12] Other works on aligned multi-wall carbon nanotubes [13] and semiconducting SWNTs in bundles [11, 14] show a polarization behavior consistent with bond-polarization theory [15], where different symmetry modes exhibit different polarization behaviors. The depolarization effects can be suppressed by the local electric field from other graphitic layers or by neighboring SWNTs.

CONCLUSION

In summary, we present here resonance Raman spectra on the graphite-like G band for isolated SWNTs, showing the G band lineshape dependence on nanotube diameter. The dispersive/non-dispersive behavior of ω_G^-/ω_G^+ can be understood based on the circumferential/axial direction for the atomic vibrations. We also present polarization studies showing that symmetry selection rules can be observed for light almost crossed to the nanotubes, and that the usual dipolar antenna behavior is suppressed when two nanotubes are resonant in the same light spot. These results explain contradictory experimental results in the literature about polarization based Raman experiments on SWNT bundles.

ACKNOWLEDGMENTS

A. J. and A.G.S.F. acknowledge financial support from the Brazilian agencies CNPq and CAPES. The MIT authors acknowledge support under NSF Grants DMR 01-16042, INT

98-15744, and INT 00-00408. R.S. acknowledges a Grant-in-Aid (No. 13440091) from the Ministry of Education, Japan. We acknowledge the NSF/CNPq joint collaboration program that makes possible exchange trips between MIT and UFMG researchers (No. NSF INT 00-00408 and No. CNPq 910120/99-4).

REFERENCES

[1] M. S. Dresselhaus, G. Dresselhaus, and P. C. Eklund, *Science of Fullerenes and Carbon Nanotubes* (Academic Press, New York, NY, San Diego, CA, 1996).

[2] M. S. Dresselhaus and P. C. Eklund, Advances in Physics **49**, 705–814 (2000).

[3] A. Jorio, R. Saito, J. H. Hafner, C. M. Lieber, M. Hunter, T. McClure, G. Dresselhaus, and M. S. Dresselhaus, Phys. Rev. Lett. **86**, 1118–1121 (2001).

[4] A. Jorio, A. G. Souza Filho, V. W. Brar, A. K. Swann, M. S. Ünlü, B. B. Goldberg, A. Righi, J. H. Hafner, C. M. Lieber, R. Saito, G. Dresselhaus, and M. S. Dresselhaus, Phys. Rev. B Rapid (2001). 7/31/01 submitted: MS BGR859.

[5] A. G. Souza Filho, A. Jorio, G. Dresselhaus, M. S. Dresselhaus, R. Saito, A. K. Swan, M. S. Ünlü, B. B. Goldberg, J. H. Hafner, C. M. Lieber, and M. A. Pimenta, Phys. Rev. B **64** (2001). submitted: 8/28/01: MS BH8324: accepted 9/26/01: AIP 077147PRB.

[6] A. G. Souza Filho, A. Jorio, G. Dresselhaus, M. S. Dresselhaus, Anna K. Swan, M. S. Ünlü, B. B. Goldberg, R. Saito, J. H. Hafner, C. M. Lieber, and M. A. Pimenta, Phys. Rev. B (2001). submitted: 5/23/01: MS BE8318; resubmitted: 8/07/01.

[7] A. Kasuya, Y. Sasaki, Y. Saito, K. Tohji, and Y. Nishina, Phys. Rev. Lett. **78**, 4434 (1997).

[8] S. D. M. Brown, A. Jorio, P. Corio, M. S. Dresselhaus, G. Dresselhaus, R. Saito, and K. Kneipp, Phys. Rev. B **63**, 5414 (2001).

[9] A. Jorio, A. G. Souza Filho, G. Dresselhaus, M. S. Dresselhaus, A. K. Swan, B. Goldberg, M. S. Ünlü, M. A. Pimenta, J. H. Hafner, C. M. Lieber, and R. Saito, Phys. Rev. B (2001). BF8180; submitted 6/14/01: resubmitted 10/13/01.

[10] S. Reich, C. Thomsen, and P. Ordejón, Phys. Rev. B **64**, 195416 (2001).

[11] A. Jorio, G. Dresselhaus, M. S. Dresselhaus, M. Souza, M. S. S. Dantas, M. A. Pimenta, A. M. Rao, R. Saito, C. Liu, and H. M. Cheng, Phys. Rev. Lett. **85**, 2617–2620 (2000).

[12] J. Hwang, H. H. Gommans, A. Ugawa, H. Tashiro, R. Haggenmueller, K. I. Winey, J. E. Fischer, D. B. Tanner, and A. G. Rinzler, Phys. Rev. B **62**, R13 310 (2000).

[13] A. M. Rao, A. Jorio, M. A. Pimenta, M. S. S. Dantas, R. Saito, G. Dresselhaus, and M. S. Dresselhaus, Phys. Rev. Lett. **84**, 1820–1823 (2000).

[14] C. Fantini, M. A. Pimenta, M. S. S. Dantas, D. Ugarte, A. M. Rao, A. Jorio, G. Dresselhaus, and M. S. Dresselhaus, Phys. Rev. B **63**, 1405 (2001).

[15] R. Saito, T. Takeya, T. Kimura, G. Dresselhaus, and M. S. Dresselhaus, Phys. Rev. B **57**, 4145–4153 (1998).